Geochemical Journal, Vol. 43, pp. 37 to 47, 2009

Oxidative scavenging of cerium on hydrous Fe oxide: Evidence from the distribution of rare earth elements and yttrium between Fe oxides and Mn oxides in hydrogenetic ferromanganese crusts

MICHAEL BAU* and ANDREA KOSCHINSKY

Earth & Space Sciences Program, School of Engineering and Science, Jacobs University Bremen, P.O. Box 750581, D-28725 Bremen, Germany

(*Received April 1, 2008; Accepted August 28, 2008*)

The distribution of the rare earths and yttrium (REY) in co-existing hydrous Mn oxides and Fe oxides that form marine hydrogenetic ferromanganese crusts is used to better describe the partitioning and fractionation of the REY between these (hydr)oxides and seawater in the natural marine system. Four fractions (easily exchangeable, Mn-oxide-bound, Fe-oxide-bound, and insoluble-residue-bound REY) were separated by an adjusted sequential leaching procedure from two ferromanganese crusts from the Central Pacific. The distribution of the REY differs significantly between these leaching fractions and gives evidence for decoupling of La, Ce, Gd, Y, and Lu from their respective neighbours in the REY series during partitioning between hydrous Fe oxides, Mn oxides and seawater. Both the Mn oxides and the Fe oxides display pronounced positive Ce anomalies of almost similar size. This suggests that in the natural marine system oxidative scavenging of Ce from seawater is not restricted to Mn oxides but also occurs on hydrous Fe oxides. The distribution of Ce between the Mn oxides and the hydrous Fe oxides follows that of the trivalent REY and contrasts sharply with that of tetravalent Zr, Hf and Th. This suggests that preferential Ce removal from seawater does not result from the oxidation of dissolved Ce(III) within the marine water column, but that Ce(III) is oxidized *after* its sorption at the metal (hydr)oxide surface. Patterns of apparent hydrous Fe oxide/Mn oxide distribution coefficients show a sigmoidal shape and display negative anomalies for La, Gd, Y, and Lu (and the M-type lanthanide tetrad effect), indicating preferential scavenging of these elements by the Mn oxides as compared to the Fe oxides. The pronounced differences between the REY distribution in the Mn oxides and that in the Fe oxides cannot solely be explained by the REY speciation in seawater, but require additional and mineral-specific REY fractionation during surface-complexation.

Keywords: rare earth elements, yttrium, ferromanganese crust, Fe oxide, Mn oxide, Ce oxidation, seawater

INTRODUCTION

Studies of trace metal scavenging by marine hydrogenetic ferromanganese (Fe–Mn) crusts suggest mineral-specific selective trace element uptake by the hydrous Fe oxides and Mn oxides these crusts are composed of (Li, 1981, 1982, 1991; Koschinsky and Halbach, 1995; Koschinsky and Hein, 2003; and references therein). As a first approximation, this selectivity has been related to the charge of the dominant dissolved species of the respective element and the surface-charge of the sorbent. We will refer to this "simplified electrostatic" model as the SES model in which positively charged dissolved species preferentially associate with the Mn oxides that have a negative surface-charge in seawater, whereas negatively charged and uncharged dissolved species prefer the slightly positively surface-charged Fe oxides.

*Corresponding author (e-mail: m.bau@jacobs-university.de)

For the rare earths and yttrium (REY) it has been suggested that both Mn oxides and Fe oxides are important REY scavengers in seawater, but that oxidative scavenging of dissolved Ce, which is the cause for the occurrence of Ce anomalies in seawater and chemical sediments (including Fe–Mn crusts) is restricted to Mn oxides (e.g., Elderfield, 1988; Moffett, 1990; and references therein). This view has been challenged by Haley *et al*. (2004) who suggested that rare earth element (REE) scavenging by marine Mn oxides is negligible and that organic coatings (referred to as "POC") and hydrous Fe oxides are the important carriers of REE(III) in the ocean. They also suggest that Ce(IV) is not associated with (hydrous) metal oxide particles but forms as a discrete Ce(IV) oxide solid phase in the water column.

Here, we present results from sequential leaching experiments performed on hydrogenetic Fe–Mn crusts in order to determine the respective amounts of REY associated with the hydrous Mn oxides and Fe oxides. Sequential leaching procedures have been widely used for the stepwise dissolution of mineral phases in composite

materials such as soils, sediments, and Fe–Mn nodules and crusts to investigate element associations (e.g., Chester and Hughes, 1967; Tessier *et al*., 1979). Although the selectivity of the leaching steps for discrete phases has sometimes been disputed, it could be shown that a thorough adaption of the leaching steps to the sample matrix provides reasonable and reproducible results for element associations in Fe–Mn crusts and nodules (Moorby and Cronan, 1981; Koschinsky and Halbach, 1995). The advantages and shortcomings of sequential leaching of Fe–Mn crusts have been discussed in detail by Koschinsky and Hein (2003) who reported the respective association of about 40 elements (excluding the REY) with the hydrous Mn oxide and Fe oxide phases and discussed these in terms of the SES model outlined earlier. However, one may argue that these studies compared elements of very different properties and geochemical behaviour. Hence, it is desirable to confirm these observations by investigating a set of trace elements, such as the REY, that behave coherently in geochemical systems.

Marine hydrogenetic Fe–Mn crusts form when hydrous Fe oxide particles and hydrous Mn oxide particles that precipitated in the water column, settle to the seafloor and build (hydr)oxidic Fe–Mn encrustrations on whatever substrate rock they are deposited on. The REY in these Fe–Mn crusts are scavenged from ambient seawater by surface-complexation on the Mn oxides and hydrous Fe oxides (e.g., Bau *et al*., 1996). While REY speciation in particle-free seawater is dominated by complexation with dissolved carbonate, this is different in the immediate vicinity of, for example, (hydrous) Fe oxide and Mn oxide particles, where the hydroxyl groups at the particle surface compete with the dissolved carbonate ligands. The result is continuous sorption and desorption of REY at or from the Mn oxide and Fe oxide particle surfaces even after the exchange equilibrium between the solution- and the surface-complexes has been reached. This continuous re-equilibration between Fe–Mn crust and ambient seawater results in the same Nd isotopic composition of the surface layer of a hydrogenetic Fe–Mn crust and ambient seawater (e.g., Albarede and Goldstein, 1992; Bau and Koschinsky, 2006; and references therein). We argue that, therefore, the REY pattern of the Mn oxide and that of the hydrous Fe oxide represent the exchange equilibrium in the three-component system Mn oxide–Fe oxide–seawater. Sequential leaching of hydrogenetic Fe–Mn crusts, which reveals the respective REY signature of the Mn oxide and the Fe oxide, allows us to study the partitioning of REY between these *co-existing* Mn oxides and Fe oxides and seawater. Our results for co-existing metal (hydr)oxides in a natural system, therefore, complement the numerous experimental studies (Byrne and Kim, 1990; Koeppenkastrop and De Carlo, 1992, 1993; De Carlo *et al*., 1998; Bau, 1999; Kawabe *et al*., 1999a, b; Ohta and Kawabe, 2000, 2001; Davranche *et al*., 2004, 2005, 2008; Verplanck *et al*., 2004; Quinn *et al*., 2004, 2006a, 2006b, 2007) that focused on REY partitioning between seawater or other solutions and either pure Mn oxides or pure (hydrous) Fe oxides. If the SES model is a reasonably good approximation, the REY should display an association with the in seawater slightly positively surface-charged Fe oxides and the negatively surface-charged Mn oxides that reflects their distribution between their dominant dissolved species in seawater, i.e., between $REYCO_3^+$ and $REY(CO_3)_2^-$.

Our results demonstrate that in the natural marine system oxidative scavenging of Ce is not limited to Mn oxides but does also occur on hydrous Fe oxides. Our results further reveal distinct and systematic differences between the REY distribution of the hydrous Fe oxide and the Mn oxide component in marine Fe–Mn crusts, which suggests that the SES model cannot fully explain or predict the behaviour of elements with complex seawater speciation during scavenging by Fe–Mn crusts.

Samples and Methods

Samples

Two non-phosphatized hydrogenetic Fe–Mn crusts were chosen for the leaching experiments. Crust 333 (c333) was sampled at about 1600 m water depth in the northern Central Pacific (15°42.07′ N, 170°21.37′ W; sampling station 64DSK, cruise SO46), crust 506 (c506) was recovered at about 1500 m water depth in the equatorial Central Pacific in the region of Kiribati (4°10.14′ S, 174°51.21′ W; sampling station 10DSR, cruise SO66). Both crusts show all the mineralogical and chemical characteristics that are typical of hydrogenetic Fe–Mn crusts. They display Mn/Fe ratios above unity (c506: 1.7; c333: 1.6) and high concentrations of Co (about 0.8%) and Ni (about 0.6%), for example. Mineralogically, they are dominated by an amorphous FeOOH phase that is closely intergrown with Fe-bearing vernadite (δ-MnO_2). The latter is an X-ray-amorphous hydrous manganese oxide (Bolton *et al*., 1988; Hein *et al*., 1997; Usui and Someya, 1997) with the chemical formula $(Mn^{4+},Fe^{3+},Ca^{2+},Na^{+})(O,OH)_2 \times nH_2O$ (Anthony *et al*., 1997), indicating that Fe and Ca are structural parts of this Mn oxide. This Fe vernadite has a hybrid structure with coexisting Mn^{4+} and Fe^{3+} domains. In one domain, Mn atoms are distributed layerwise, as in phyllomanganate, whereas in the other, Fe octahedra are linked as in feroxyhite (Manceau *et al*., 1992).

Methods

The ground (<63 μm) and air-dried Fe–Mn crust samples were sequentially leached following the well-established protocol of Koschinsky and Halbach (1995). A 1 g sample aliquot was put in a 250 ml NALGENE

polyethylene bottle, the leaching reagent was added, and the suspension was shaken on a horizontal shaker. The leaching solution was filtered through a 0.45 μm membrane filter and the filtrate stored for analysis. The solid remaining on the filter was rinsed twice with deionized water and then immediately transferred to the next leaching step. The following four fractions were separated:

Leach 1: easily leachable adsorbed cations and carbonates acid-leachable with 25 ml of a 1 M acetate buffer at pH 5;

Leach 2: Mn oxide fraction easily reducible with 175 ml of a 0.1 M hydroxylamine hydrochloride solution at pH 2;

Leach 3: hydrous Fe oxide fraction moderately reducible with 175 ml of a 0.2 M oxalate buffer solution at pH 3.5;

Leach 4: residual fraction with (alumino)silicates, crystalline oxides, etc., dissolved in concentrated HF, HNO_3 and HCl in an acid-pressure digestion system.

The resulting leaching solutions were acidified with HNO_3 to pH 2 for storage and subjected to major/minor and trace metal analyses with a Leeman ICP-OES and a PerkinElmer/Sciex Elan 5000 ICP-MS (for details see Koschinsky and Halbach, 1995, Bau *et al*., 1996).

Results and Assessment of Separation Efficiency

The results of the sequential leaching procedure are compiled in Table 1 and are illustrated in Fig. 1. The equations for the quantification of anomalies in normalized REY patterns are given in Table 1; note that these data have been calculated using shale-normalized REY data.

Leaching fraction 1 (commonly referred to as the fraction representing carbonates and loosely bound elements) contains about 55% of total Ca and only insignificant amounts (<0.1%) of total Mn and total Fe. Moreover, it carries only a small fraction (1.9–7.4%) of the total REY budget of the hydrogenetic Fe–Mn crusts (Table 1). The REY_{SN} patterns ("SN" indicates normalization to Post-Archean Australian Shale from McLennan, 1989) are characterized by light REE (LREE) depletion and only little fractionation between middle and heavy REE (MREE and HREE, respectively). The REY_{SN} patterns (Fig. 1) show pronounced negative Ce anomalies (Ce_{SN}/Ce^* = 0.11; 0.09), positive anomalies for La (La_{SN}/Ce^* = 2.06; 2.80), Gd (Gd_{SN}/Gd^* = 1.55; 1.57) and Lu (Lu_{SN}/Yb_{SN} = 1.21; 1.21), and very small anomalies for Y (Y_{SN}/Ho_{SN} = 1.07; 1.11).

Leaching fraction 2 (containing the elements associated with the Fe-bearing Mn oxide vernadite) hosts almost the entire amount (98.4%) of total Mn, but also about 44.4% (c506) and 42.9% (c333) of total Ca, and 29.8% (c506) and 18.5% (c333) of total Fe. Leaching solution 2

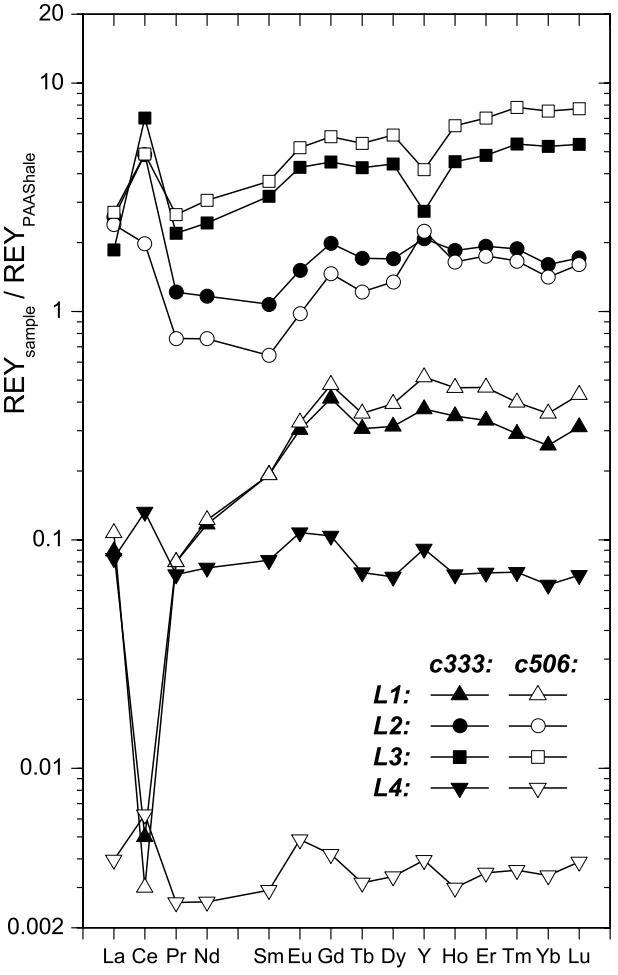

Fig. 1. REY_{SN} patterns of (L1) the easily accessible trace element fraction, (L2) the Fe-bearing Mn oxide fraction, (L3) the amorphous hydrous Fe oxide fraction, and (L4) the residual fraction in marine hydrogenetic Fe–Mn crusts c333 and c506. While REY concentrations and REY_{SN} patterns differ significantly between these four fractions, there are only insignificant differences between the respective fractions in the two crusts c333 and c506.

also contains 14% to 56% of the total REY (Table 1). The REY_{SN} pattern of fraction 2 (Fig. 1) is flat between the LREE and MREE, increases within the MREE and is flat again between the MREE and HREE. There are positive anomalies for La (La_{SN}/Ce^* = 2.05; 3.14), Ce (Ce_{SN}/Ce^* = 3.87; 2,59), Gd (s/Gd* = 1.33; 1.57), Y (Y_{SN}/Ho_{SN} = 1.13; 1.37), and Lu (Lu_{SN}/Yb_{SN} = 1.07; 1.14).

Leaching fraction 3 (containing the elements associated with amorphous (hydrous) Fe oxides) yields 67.6% (c506) and 81.2% (c333) of total Fe and only insignificant amounts (<2%) of Mn and Ca. This fraction carries between 40% and 82% of the total REY (Table 1). The REY_{SN} patterns of this fraction (Fig. 1) increase from the

Table 1. Major and trace element concentrations in the four leaching fractions of Fe–Mn crusts c333 and c506 and the relative distribution of REY between these four fractions

	333-1	333-2	333-3	333-4	333-tot	506-1	506-2	506-3	506-4	506-tot
[%]										
Ca	1.51	1.17	0.05	<0.01	2.73	1.59	1.32	0.06	<0.01	2.97
Mn	0.02	27.1	0.41	<0.01	27.53	0.02	24	0.36	<0.01	24.38
Fe	0.03	3.24	14.2	0.03	17.5	0.03	4.39	9.95	0.35	14.72
[μg/g]										
Rb	1.5	1.36	0.17	1.19	4.22	1.31	1.04	0.09	0.11	2.55
Sr	aud	726	12.9	12.1		aud	799	9.02	1.94	
Zr	0.2	<0.5	626	5.16	631	0.16	<0.5	534	0.69	535
Cs	0.004	0.019	<0.01	0.06	0.083	0.004	<0.05	<0.01	<0.01	0.004
Ba	7.11	1464	315	17.5	1804	6	1318	147	1.73	1473
Hf	<0.03	<0.2	9.85	0.16	10.01	<0.03	<0.2	7.14	<0.5	7.14
Pb	<0.02	31.7	1223	26.5	1281	<0.02	9.88	1181	1.11	1192
Th	<0.02	<0.1	6.44	0.07	6.51	<0.02	<0.1	3	<0.1	3
U	5.41	0.05	8	0.027	13.49	6.48	0.04	7.77	0.003	14.29
Y	10.1	56.2	74.1	2.46	142.86	13.9	60.8	112.5	0.107	187.31
La	3.39	98.7	71	3.17	176.26	4.1	91.4	104	0.151	199.65
Ce	0.382	388	559	10.5	957.88	0.262	157	388	0.499	545.76
Pr	0.705	10.7	19.4	0.623	31.43	0.706	6.71	23.4	0.0228	30.84
Nd	3.95	39.5	82.6	2.55	128.60	4.12	25.7	104	0.088	133.91
Sm	1.07	5.97	17.7	0.452	25.19	1.07	3.55	20.6	0.0162	25.24
Eu	0.328	1.63	4.61	0.116	6.68	0.353	1.05	5.63	0.0053	7.04
Gd	1.94	9.26	21	0.484	32.68	2.22	6.83	27.1	0.0196	36.17
Tb	0.237	1.32	3.29	0.0556	4.90	0.277	0.944	4.21	0.0024	5.43
Dy	1.47	7.93	20.7	0.322	30.42	1.85	6.3	27.6	0.0157	35.77
Ho	0.345	1.83	4.49	0.0698	6.73	0.458	1.63	6.43	0.003	8.52
Er	0.95	5.49	13.8	0.204	20.44	1.32	4.98	20	0.0099	26.31
Tm	0.118	0.76	2.18	0.0292	3.09	0.161	0.673	3.17	0.0015	4.01
Yb	0.729	4.51	14.9	0.179	20.32	1.01	3.97	21.2	0.0096	26.19
Lu	0.135	0.742	2.33	0.0303	3.24	0.187	0.694	3.34	0.0017	4.22
Anomalies:										
Ce_{SN}/Ce^*	0.11	3.87	3.59	2.00	3.62	0.09	2.59	2.18	2.44	2.26
La_{SN}/Ce^*	2.06	2.05	0.95	1.26	1.39	2.80	3.14	1.22	1.54	1.72
Gd_{SN}/Gd^*	1.55	1.33	1.16	1.38	1.22	1.57	1.43	1.19	1.38	1.25
Lu_{SN}/Yb_{SN}	1.21	1.07	1.02	1.10	1.04	1.21	1.14	1.03	1.15	1.05
Y_{SN}/Ho_{SN}	1.07	1.13	0.61	1.29	0.78	1.11	1.37	0.64	1.31	0.81
[%]										
Y	7.07	**39.34**	**51.87**	1.72	100.00	7.42	**32.46**	**60.06**	0.06	100.00
La	1.92	**56.00**	**40.28**	1.80	100.00	2.05	**45.78**	**52.09**	0.08	100.00
Ce	0.04	**40.51**	**58.36**	1.10	100.00	0.05	**28.77**	**71.09**	0.09	100.00
Pr	2.24	**34.05**	**61.73**	1.98	100.00	2.29	**21.76**	**75.88**	0.07	100.00
Nd	3.07	**30.72**	**64.23**	1.98	100.00	3.08	**19.19**	**77.67**	0.07	100.00
Sm	4.25	**23.70**	**70.26**	1.79	100.00	4.24	**14.07**	**81.63**	0.06	100.00
Eu	4.91	**24.39**	**68.97**	1.74	100.00	5.02	**14.92**	**79.99**	0.08	100.00
Gd	5.94	**28.33**	**64.25**	1.48	100.00	6.14	**18.88**	**74.92**	0.05	100.00
Tb	4.83	**26.92**	**67.11**	1.13	100.00	5.10	**17.37**	**77.48**	0.04	100.00
Dy	4.83	**26.07**	**68.04**	1.06	100.00	5.17	**17.61**	**77.17**	0.04	100.00
Ho	5.12	**27.17**	**66.67**	1.04	100.00	5.37	**19.13**	**75.46**	0.04	100.00
Er	4.65	**26.85**	**67.50**	1.00	100.00	5.02	**18.93**	**76.02**	0.04	100.00
Tm	3.82	**24.62**	**70.61**	0.95	100.00	4.02	**16.80**	**79.14**	0.04	100.00
Yb	3.59	**22.20**	**73.33**	0.88	100.00	3.86	**15.16**	**80.95**	0.04	100.00
Lu	4.17	**22.92**	**71.97**	0.94	100.00	4.43	**16.43**	**79.10**	0.04	100.00

aud = above upper limit of determination.
$Ce^* = 2Pr–Nd$; $Gd^* = 0.33Sm + 0.67Tb$ (Pr, Nd, Sm, Tb: shale-normalized data).

LREE over the MREE to the HREE. There are positive Ce (Ce_{SN}/Ce^* = 3.59; 2.18) and Gd anomalies (Gd_{SN}/Gd^* = 1.16; 1.19) and negative Y anomalies (Y_{SN}/Ho_{SN} = 0.61; 0.64), and no Lu anomalies (Lu_{SN}/Yb_{SN} = 1.02; 1.03). While c506 shows a positive La anomaly (La_{SN}/Ce^* = 1.22), c333 does not (La_{SN}/Ce^* = 0.95).

Leaching fraction 4 (commonly addressed as the residual fraction that comprises detrital aluminosilicates, crystalline Fe oxides and accessories such as apatite, opal, and barite) hosts only insignificant amounts (<0.1%) of Ca and Mn, and only a very small fraction (c506: 2.4%; c333: 0.2%) of total Fe. Leaching solution 4 shows a negligible fraction (0–1.7%) of the total REY budget of these non-phosphatized hydrogenetic Fe–Mn crusts (Table 1). The REY_{SN} patterns of this fraction (Fig. 1) are flat, but show positive anomalies for La (La_{SN}/Ce^* = 1.26; 1.54), Ce (Ce_{SN}/Ce^* = 2.00; 2.44), Gd (Gd_{SN}/Gd^* = 1.38; 1.38), and Y (Y_{SN}/Ho_{SN} = 1.29; 1.31).

The distribution of the major elements Ca, Mn and Fe demonstrates that the sequential leaching approach applied here successfully separated the element pool associated with the Fe-bearing Mn oxide (vernadite) and that bound to the hydrous Fe oxide. Leaching solution 3 is rich in Fe but very low in Ca and Mn, and shows an Fe/Mn ratio of 28 and 35, respectively. Its REY load, therefore, represents only those REY that are associated with the hydrous Fe oxides. Leaching solution 2 carries not only Mn but also Fe and Ca. Vernadite, however, is known to readily accommodate divalent and trivalent cations, such as Ca and Fe, respectively, in its crystal lattice (as discussed earlier), and hence, this is to be expected. Moreover, it had previously been shown that the amount of Fe leached with step 2 does *not* correlate with the total Fe content of a Fe–Mn crust, but with its total Mn content (Koschinsky and Halbach, 1995). Together with the mineralogical structure of vernadite (discussed in Subsection "Samples"), this suggests that the Fe present in leaching solution 2 is the Fe hosted by the Fe-bearing vernadite, and that it does not represent Fe mobilized from the hydrous Fe oxide phase that is leached in step 3. Although the leaching solution 1 carries most of the Ca, its REY_{SN} patterns are significantly different from those of marine limestones, suggesting that the REY in fraction 1 are derived from an ill-defined easily accessible trace element pool and not exclusively from carbonates.

Since neither leaching fraction 1 nor fraction 4 carries significant amounts of REY (Table 1), further discussion will focus on leaching solutions 2 and 3, i.e., on the Mn oxides and the hydrous Fe oxides, that are the important REY carriers. Since we will specifically address the behaviour of redox-sensitive Ce relative to its redox-insensitive REE neighbour Pr, we emphasize that 98.9% and 99.9% of total Ce, and 95.9% and 97.8% of total Pr are associated with the (hydrous) Fe and Mn oxides in c333 and c506, respectively. Also note that the REY patterns of the bulk hydrogenetic Fe–Mn crusts studied here do not differ from those considered typical of hydrogenetic Fe–Mn crusts. The different size of the positive Ce anomalies in the bulk hydrogenetic Fe–Mn crusts c333 and c506 (Table 1) results from the different average growth rates of these two crusts (Kuhn *et al*., 1998).

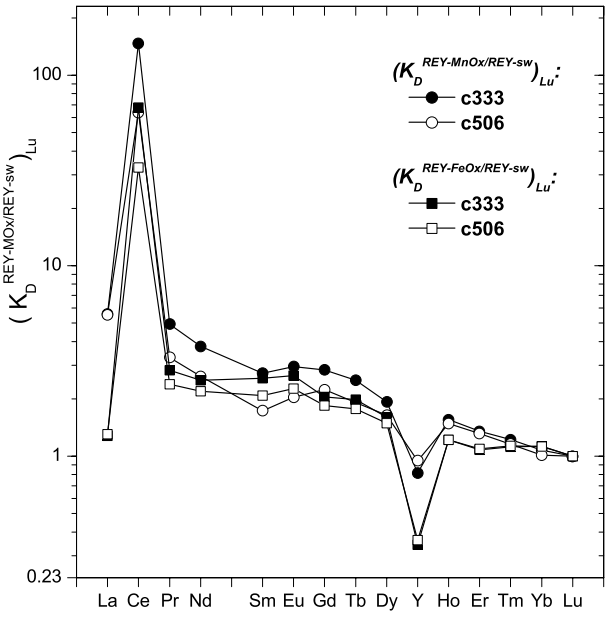

Fig. 2. Patterns of $(K_D^{REY\text{-}MnOx/REY\text{-}sw})_{Lu}$ and of $(K_D^{REY\text{-}FeOx/REY\text{-}sw})_{Lu}$ values for hydrogenetic Fe–Mn crusts c333 and c506, calculated following Eqs. (1a) and (1b) and using Central Pacific seawater data from Zhang and Nozaki (1996). All patterns are characterized by HREE depletion, positive Ce anomalies of similar size and negative Y anomalies that are strongest in the hydrous Fe oxide. Patterns of $(K_D^{REY\text{-}FeOx/REY\text{-}sw})_{Lu}$ also display negative La and small negative Gd anomalies. Redox-sensitive Ce does not show any preference for the Mn oxide, but was also oxidatively scavenged by the hydrous Fe oxides. In contrast, fractionation of non-redox-sensitive REY appears to be more pronounced on the hydrous Fe oxides than on the Mn oxides.

DISCUSSION

Cerium oxidation in the marine environment

It has been suggested that the behaviour of Ce in the marine environment is more closely coupled to that of Mn than to that of Fe, due to oxidative scavenging of Ce by Mn oxides (e.g., Elderfield, 1988). Thermodynamics suggest that Ce(IV) should predominate over Ce(III) at redox levels that stabilize significant amounts of (hydr)oxides of Fe(III), Mn(III), or Mn(IV), and it has been shown that the slow kinetics of the Ce(III) oxidation reaction can be overcome by microbial mediation or

by surface-catalyses on Mn oxides (e.g., Moffett, 1990, 1994; Koeppenkastrop and De Carlo, 1992; De Carlo *et al*., 1998; and references therein). If indeed there is preferential association of Ce with Mn but not with Fe, only the Mn oxides in marine hydrogenetic Fe–Mn crusts should display a positive Ce anomaly when compared to seawater which itself is characterized by Ce depletion.

The oxidative scavenging of Ce by *co-existing* Mn oxides and hydrous Fe oxides in hydrogenetic Fe–Mn crusts (i.e., the decoupling of Ce from its REY neighbours) is illustrated in Fig. 2 by the Lu-normalized apparent mineral/seawater partition coefficients for the REY, $(K_D^{\text{REY-MnOx/REY-sw}})_{\text{Lu}}$ and $(K_D^{\text{REY-FeOx/REY-sw}})_{\text{Lu}}$, respectively (seawater is Central Pacific seawater (00°00.54′ S, 149°57.34′ E) from 1486 m depth from Zhang and Nozaki, 1996):

$$(K_D^{\text{REY-MnOx/REY-sw}})_{\text{Lu}} = ([\text{REY}]_{\text{MnOx}}/[\text{REY}]_{\text{sw}})/([\text{Lu}]_{\text{MnOx}}/[\text{Lu}]_{\text{sw}}), \quad (1a)$$

$$(K_D^{\text{REY-FeOx/REY-sw}})_{\text{Lu}} = ([\text{REY}]_{\text{FeOx}}/[\text{REY}]_{\text{sw}})/([\text{Lu}]_{\text{FeOx}}/[\text{Lu}]_{\text{sw}}). \quad (1b)$$

Straightforward inspection of the patterns in Fig. 2 reveals that both the K_D patterns of the Mn oxides and those of the hydrous Fe oxides, display strong positive Ce anomalies. This is evidence from a natural system that the preferential association of Ce (relative to the non-redox-sensitive REY) with metal (hydr)oxides is not restricted to Mn oxides, but that this can also be observed on hydrous Fe oxides. This observation is in agreement with experimental results that suggested oxidative Ce scavenging by hydrous Fe oxides from dilute HCl solutions (Bau, 1999). However, the majority of experimental studies (Byrne and Kim, 1990; Koeppenkastrop and De Carlo, 1992, 1993; De Carlo *et al*., 1998; Kawabe *et al*., 1999a, b; Ohta and Kawabe, 2000, 2001; Verplanck *et al*., 2004; Davranche *et al*., 2004; Quinn *et al*., 2004, 2006a, 2006b, 2007) did not find evidence of preferential Ce scavenging, although some of the data sets presented, such as those of Verplanck *et al*. (2004) and Davranche *et al*. (2004), for example, show very small positive Ce anomalies in patterns of Fe-(hydr)oxide/solution partition coefficients. Hence, the claim of preferential (oxidative) scavenging of Ce by hydrous Fe oxides is still considered controversial and is not widely accepted. One might argue that the observed discrepancy results from comparing experiments in which the REY are scavenged *during* the precipitation of Fe and Mn (hydr)oxides (as in the study by Bau, 1999) with experiments where the REY are added to pre-existing Fe and Mn (hydr)oxides. However, even in the study of Bau (1999) only the experiments with artificial solutions showed oxidative Ce scavenging, whereas those using acidified Fe-rich natural spring water from Nishiki-numa, Hokkaido, Japan (Bau *et al*., 1998), did not. This clearly demonstrates that further experimental work is needed to shed light on this issue. We emphasize, though, that despite the obvious disagreement between most experimental results and our findings, the data reported here represent an observation in the natural marine system and that our results most strongly suggest that oxidative scavenging of Ce by hydrous Fe oxide does indeed occur in nature.

Due to decoupling of La from its neighbours in the REY series (which is also evident in Fig. 2), Ce anomalies in marine chemical sediments should not be quantified by interpolation between its neighbours La and Pr (Bau and Dulski, 1996). Several alternative approaches have been proposed (e.g., Bau and Dulski, 1996; Bolhar *et al*., 2004) and we here use the Ce_{SN}/Ce^* ratio (Bolhar *et al*., 2004; Table 1) and the Ce/Pr ratio of the partition coefficients calculated from Eqs. (1a) and (1b) to quantify decoupling of redox-sensitive Ce from its trivalent-only LREE neighbours. The Ce/Pr ratios of the partition coefficients for c333 are 58 and 46 for the Mn oxides and the Fe oxides, respectively, whereas those for c506 are 37 and 27, respectively, i.e., Ce enrichment in the Fe oxides is only 21% (c333) and 27% (c506) smaller than it is in the Mn oxides. When we quantify Ce decoupling by the Ce_{SN}/Ce^* ratio this difference is even smaller: 7% (c333) and 15% (c506). This indicates that preferential (i.e., oxidative) scavenging of Ce from seawater by hydrous Fe oxides is not minute, but that it is almost as effective as Ce scavenging by Mn oxides.

Our result of Ce enrichment in *both* the Mn oxide and the hydrous Fe oxide fraction also suggests that the transfer of Ce from seawater into sediments does not occur via a discrete solid Ce(IV) oxide phase, such as CeO_2, that forms from oxidation of dissolved Ce(III) within the marine water column. For the sake of the argument let us assume such a hypothetical phase existed: If this discrete Ce(IV) phase was soluble in 0.1 M hydroxylamine hydrochloride solution at pH 2 (leaching step 2) or in both 0.1 M hydroxylamine hydrochloride solution at pH 2 and 0.2 M oxalate buffer solution at pH 3.5 (step 2 and 3, respectively), this Ce(IV) phase would dissolve with the Mn oxides and we would have found the positive Ce anomaly only in the Mn oxide fraction. If this hypothetical Ce(IV) oxide phase was soluble in step 3 but not in step 2, only the hydrous Fe oxide fraction would have displayed a positive Ce anomaly. If this phase was insoluble during both leaching steps, neither the hydrous Fe oxide nor the Mn oxide fraction would have shown a positive Ce anomaly, but leach 4 would have done so. That about half of this hypothesized Ce(IV) oxide phase should be soluble in step 2 and the other half in step 3 is very unlikely. Hence, the observed preferential enrich-

ment of Ce in *both* the Mn oxide and the hydrous Fe oxide fraction (Fig. 2), does not support the conclusion that Ce precipitates as a separate Ce(IV) oxide phase in the water column. Instead, it obviously indicates that Ce(IV) is indeed associated with both the hydrous Fe oxide *and* the Mn oxide particles.

It might be argued that a discrete Ce(IV) oxide compound forms via oxidation of dissolved Ce(III) within the marine water column, but subsequently associates with Mn and Fe (hydr)oxide particles and is eventually deposited together with these Mn and Fe (hydr)oxides to produce hydrogenetic Fe–Mn crusts. However, using the marine behaviour of non-redox-sensitive *tetra*valent cations as a guidance, this is very unlikely. Tetravalent Zr, Hf, and Th, for example, behave very different from Ce: while Ce in Fe–Mn crusts is distributed almost equally between the Mn oxides and the hydrous Fe oxides (Table 1), Zr, Hf and Th are bound *exclusively* to the hydrous Fe oxide phase (Bau and Koschinsky, 2006; see also Table 1). Hence, the general distribution of Ce between the Mn oxides and the Fe oxides in a hydrogenetic Fe–Mn crust is similar to that of the redox-insensitive trivalent REY, but distinctly different from that of Zr(IV), Hf(IV) and Th(IV).

Our results, therefore, strongly suggest that discrete Ce(IV) (hydr)oxide compounds do not form via the oxidation of dissolved Ce(III) *within* the marine water column, but that Ce dissolved in seawater is trivalent and distributed between mono- and dicarbonate complexes just as its REE(III) neighbours. The oxidation of Ce(III) and the formation of Ce(IV) compounds happens *at the surface* of marine hydrous Mn *and* Fe oxides *after* the initial sorption of Ce(III).

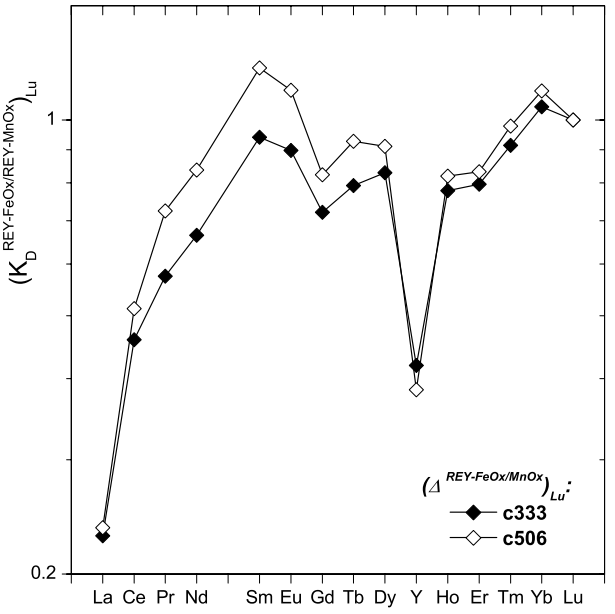

Fig. 3. Patterns of $(\Delta^{REY\text{-}FeOx/REY\text{-}MnOx})_{Lu}$ values for hydrogenetic Fe–Mn crusts c333 and c506, calculated following Eq. (2). The patterns display a sigmoidal shape with the M-type lanthanide tetrad effect and negative anomalies of La, Gd, Y, and Lu, but no anomaly for Ce. The latter corroborates the lack of preferential oxidative scavenging of Ce on Mn oxide, whereas the former indicate preferential partitioning of La, Gd, Y, and Lu onto the Mn oxides. The fact that the patterns differ from a flat line demonstrates that REY sorption characteristics of Mn oxide and on hydrous Fe oxide particles in seawater are different and that these particles, therefore, are not covered by organic coatings or biofilms that create a uniform negative surface-charge.

REY fractionation between co-existing Mn oxides and hydrous Fe oxides in seawater

To illustrate the differences between the REY distribution in the hydrous Mn oxides and Fe oxides present in hydrogenetic Fe–Mn crusts, we calculated the Lu-normalized ratio of Fe-bound REY (leaching step 3) to Mn-bound REY (leaching step 2) for the members of the REY series (Fig. 3):

$$(\Delta^{REY\text{-}FeOx/REY\text{-}MnOx})_{Lu} = ([REY]^{FeOx}/[REY]^{MnOx})/([Lu]^{FeOx}/[Lu]^{MnOx}). \quad (2)$$

The resulting patterns of $(\Delta^{REY\text{-}FeOx/REY\text{-}MnOx})_{Lu}$ values are very similar for both crusts and display a sigmoidal shape. Compared to their respective neighbours in the REY series, La, Gd, Y and Lu preferentially associate with the Mn oxide as demonstrated by the negative anomalies for these elements in Fig. 3. Moreover, the patterns in Fig. 3 are subdivided into four convex segments resembling the M-type lanthanide tetrad effect (Masuda *et al.*, 1987). We also emphasize again the lack of any Ce anomaly from the patterns in Fig. 3, which indicates that there is no preferential oxidative scavenging of Ce by Mn oxides as compared to hydrous Fe oxides, as was discussed in Subsection "Cerium oxidation in the marine environment".

The patterns of the Fe-hydroxide/Mn-oxide distribution factors (Fig. 3) demonstrate that although the Mn oxides and the hydrous Fe oxides are intimately associated with each other in marine hydrogenetic Fe–Mn crusts, pronounced differences exist between their respective REY distribution.

In the SES model (Li *et al.*, 1981, 1982, 1991; Koschinsky and Halbach, 1995; Koschinsky and Hein, 2003) similar differences observed for other trace elements had been attributed to differences between the seawater speciation of the elements considered and the surface charge of the hydrous Fe and Mn oxides in seawater, respectively. If the SES model can be used to approximate the behaviour of elements, such as the REY,

whose seawater speciation is split between complex species of different charge, the speciation of dissolved REY in seawater should explain the apparent $(\Delta^{\text{REY-FeOx/REY-MnOx}})_{\text{Lu}}$ values we observe (Fig. 3). Solution-complexation of REY in seawater is dominated by positively charged monocarbonate and negatively charged dicarbonate complexes, $REYCO_3^+$ and $REY(CO_3)_2^-$, respectively (e.g., Byrne and Kim, 1990). Utilizing data from Byrne (2002), we calculated the $[REY(CO_3)_2^-]/[REYCO_3^+]$ ratio in seawater of pH 8 for each member of the REY series. The REY from La to Nd preferentially occur as monocarbonate complexes, while for the rest of the series dicarbonate complexes predominate. The $[REY(CO_3)_2^-]/[REYCO_3^+]$ ratios increase along the REY series with negative "anomalies" for Gd, Y and Yb. The negative Yb "anomaly" results from an anomalously high value for β_{YbCO3} in the data set of Liu and Byrne (1998) and will not be considered any further.

Since the pattern of $[REY(CO_3)_2^-]/[REYCO_3^+]$ ratios illustrates the ratio between the dominant negatively and positively charged dissolved REY species in seawater, this pattern should resemble the patterns of $(\Delta^{\text{REY-FeOx/REY-MnOx}})_{\text{Lu}}$ values, if it is solution-speciation *alone* that controls the mineral association of the REY during scavenging from seawater. However, normalizing the $[REY(CO_3)_2^-]/[REYCO_3^+]$ ratios to the $[Lu(CO_3)_2^-]/[LuCO_3^+]$ ratio and superimposing the resulting Lu-normalized pattern onto Fig. 3 reveals only a faint similarity between the $(\Delta^{\text{REY-FeOx/REY-MnOx}})_{\text{Lu}}$ values and the distribution of dissolved REY between mono- and dicarbonate complexes in seawater (Fig. 4).

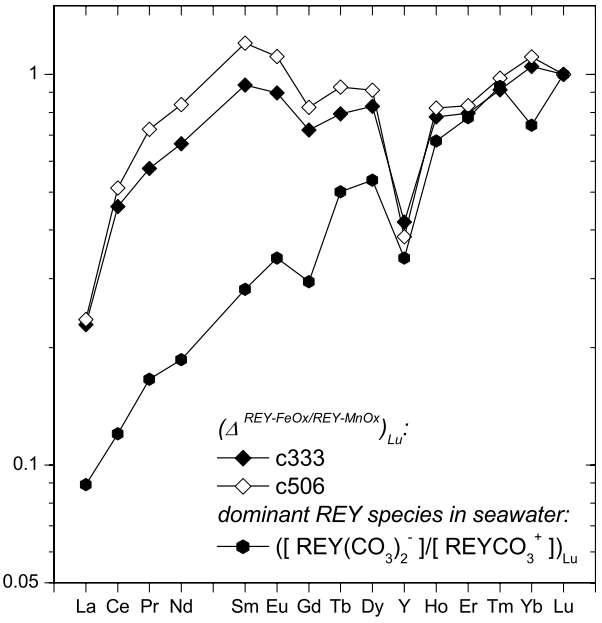

Fig. 4. Patterns of $(\Delta^{REY-FeOx/REY-MnOx})_{Lu}$ values for hydrogenetic Fe–Mn crusts c333 and c506 compared to the Lu-normalized distribution of the REY between mono- and dicarbonate complexes, $([REY(CO_3)_2^-]/[REYCO_3^+])_{Lu}$, in seawater at pH 8. The differences demonstrate that the speciation of the REY in seawater alone is not sufficient to describe the distribution of the REY between the hydrous Fe and Mn oxides in Fe–Mn crusts. They further suggest that the fractionation caused by REY surface-complexation on hydrous Fe oxides differs from that produced by REY surface-complexation on Mn oxides.

Comparison of Y and its geochemical twin Ho (Bau, 1996) also indicates that the SES model does not adequately describe REY behaviour during scavenging. In seawater of pH 8, 56% of total Y occurs a $Y(CO_3)_2^-$ complex and 44% as YCO_3^+ complex, whereas 72% of total Ho occurs as $Ho(CO_3)_2^-$ and 28% as $HoCO_3^+$ (calculated from data in Table 1 of Byrne, 2002). At pH 7.5, the respective percentages are 29% and 71% for Y, and 45% and 55% for Ho. Over the entire pH range of Fe–Mn crust forming marine environments, therefore, negatively charged dicarbonate complexes are more important for Ho than for Y, whereas in marked contrast, positively charged monocarbonate complexes are more important for Y than for Ho. Utilizing the same seawater composition (Zhang and Nozaki, 1996) as in Eqs. (1a) and (1b), the above values at pH 8 suggest that in comparison to the total seawater Y/Ho weight-ratio of 62, the Y/Ho ratio of the fraction of total seawater REY that occur as positively charged monocarbonate complexes is 98 and the Y/Ho ratio of the fraction that occurs as negatively charged dicarbonate complexes is only 45. The SES model predicts that the positively charged monocarbonate complexes should associate with the negatively surface-charged Mn oxide and that the negatively charged dicarbonate complexes should associate with the positively surface-charged hydrous Fe oxide. Thus, the Y/Ho ratio of the Mn oxides in Fe–Mn crusts should be higher than that of total seawater, because only the monocarbonate complexes are scavenged and the Y/Ho ratio of these is 98 (i.e., it is higher than the Y/Ho ratio of 62 of total seawater). In contrast, the Fe oxides should display a Y/Ho ratio that is below that of ambient seawater, because the Y/Ho ratio of the fraction occurring as dicarbonate complex is only 45 (i.e., it is smaller than that of total seawater). However, the Y/Ho ratio of the Mn oxides is 31 and 37 in c333 and c506, respectively, and the Y/Ho ratio of the Fe oxides is 17 and 18, respectively. Although the Y/Ho ratio of the Mn oxides exceeds that of the hydrous Fe oxides as predicted by the SES model, they both show Y/Ho ratios significantly lower than the Y/Ho ratio of ambient seawater, which is in marked contrast to predictions based on the SES model.

Our results indicate that while the SES model may serve as a straightforward approximation of the scavenging behaviour of elements with simple seawater

speciation, it cannot be used to comprehensively describe scavenging of elements with complex speciation, such as the REY, during formation of hydrogenetic Fe–Mn crusts. Obviously, the surface-complexation of dissolved REY with ligands (predominantly hydroxyl groups) at the oxide particle surfaces, which is significantly stronger for Ho than for Y (e.g., Byrne and Lee, 1993; Bau *et al*., 1996, 1998; Bau, 1999), promotes the preferential scavenging of Ho over Y and ultimately produces lower Y/Ho ratios in both Mn oxides and Fe oxides when compared to ambient seawater (remember that the anomalously weak surface-complexation of Y relative to Ho and its REE neighbours is the ultimate reason for the positive Y anomaly and super-chondritic Y/Ho ratio of seawater). However, the strong differences between the REY patterns of the Mn and the Fe oxides cannot be explained by REY solution-complexation alone, and hence, they suggest that REY fractionation during surface-complexation on hydrous Fe oxides differs from that on Mn oxides, supporting the findings of Quinn *et al*. (2004) who argued that in contrast to Mn oxides, REY surface-complexation on Fe (hydr)oxides cannot be approximated by the first hydrolysis constants of the REY.

The strong difference between the REY distribution in the hydrous Fe oxides and in the Mn oxides demonstrates that the surfaces of these (hydr)oxide particles have different affinities for trace elements, suggesting the absence of coatings or (bio)films that produce uniform surface properties with respect to sorption of REY. This is in marked contrast to particles in shallow open ocean, coastal and estuarine waters, that are all characterized by a negative surface charge (e.g., Neihof and Loeb, 1972; Hunter and Liss, 1979, 1982; Hunter, 1991), which has been ascribed to the presence of organic coatings and biofilms (e.g., Balistrieri *et al*., 1981).

Conclusion

Sequential leaching of marine hydrogenetic Fe–Mn crusts revealed significant differences between the REY distribution in the co-existing Mn oxide and Fe oxide fractions. Since the REY distribution in such Fe–Mn crusts represents the exchange equilibrium between the REY scavenged by these (hydr)oxide particles and the REY dissolved in ambient seawater, these data allow us to characterize REY partitioning in the system Mn oxide–Fe oxide–seawater.

The apparent mineral/seawater REY partition coefficents ($K_D^{\text{REY-MnOx/REY-sw}}$ and $K_D^{\text{REY-FeOx/REY-sw}}$, respectively) confirm the general results from a study of bulk partition coefficients (Bau *et al*., 1996), but provide clear indications for that in the natural marine system oxidative scavenging of dissolved Ce is not confined to Mn oxides but also occurs on hydrous Fe oxides. The mineral association of Ce is similar to that of the trivalent REY and different from that of tetravalent Zr, Hf, and Th. While the latter indicates that Ce oxidation does not occur in the marine water column but at the metal (hydr)oxide surface, the former suggests that if the redox level of the marine environment is high enough for Ce(III) oxidation, the oxidation reaction is catalyzed regardless of whether an Fe or Mn (hydr)oxide sorbent provides the surface sites.

The apparent Lu-normalized mineral/mineral REY fractionation factors $(\Delta^{\text{REY-FeOx/REY-MnOx}})_{\text{Lu}}$ display sigmoidal patterns that show negative anomalies for Gd, Y, Lu, and possibly La, and the M-type lanthanide tetrad effect. Hence, there exist significant differences between the REY distribution of the Fe oxides and that of the Mn oxides, which cannot be explained by the seawater speciation of the REY but requires strong fractionation during REY surface-complexation. The latter appears to be different on Mn oxides as compared to Fe oxides supporting previous suggestions by Quinn *et al*. (2004). The differences between the REY distribution in the Mn oxides and in the Fe oxides from marine hydrogenetic Fe–Mn crusts also suggests that these (hydr)oxide particles are not covered by organic coatings or biofilms, but that the inorganic (hydr)oxide surface controls the scavenging of trace elements from deep seawater.

Acknowledgments—We are very thankful for the help and the analytical expertise of Peter Dulski, GFZ Potsdam. We appreciate the helpful comments from journal reviewers O. Pourret and D. Vance and the efficient editorial handling of associate editor B. Orberger.

References

Albarede, F. and Goldstein, S. L. (1992) World map of Nd isotopes in sea-floor ferromanganese deposits. *Geology* **20**, 761–763.

Anthony, J. W., Bideaux, R. A., Bladh, K. W. and Nichols, M. C. (1997) *Handbook of Mineralogy*, Vol. 3, 595. Available at http://www.handbookofmineralogy.org/pdfs/vernadite.pdf

Balistrieri, L. S., Brewer, P. G. and Murray, J. W. (1981) Scavenging residence times of trace metals and surface chemistry of sinking particles in the deep ocean. *Deep-Sea Res.* **28**(2A), 101–121.

Bau, M. (1996) Controls on the fractionation of isovalent trace elements in magmatic and aqueous systems: Evidence from Y/Ho, Zr/Hf, and lanthanide tetrad effect. *Contrib. Mineral. Petrol*. **123**, 323–333.

Bau, M. (1999) Scavenging of dissolved yttrium and rare earths by precipitating iron oxyhydroxide: Experimental evidence for Ce oxidation, Y–Ho fractionation, and lanthanide tetrad effect. *Geochim. Cosmochim. Acta* **63**, 67–77.

Bau, M. and Dulski, P. (1996) Distribution of yttrium and rare-earth elements in the Penge and Kuruman Iron-Formations,

Transvaal Supergroup, South Africa. *Precambrian Res*. **79**, 37–55.

Bau, M. and Koschinsky, A. (2006) Hafnium and neodymium isotopes in seawater and ferromanganese crusts: the "element perspective". *Earth Planet. Sci. Lett*. **241**, 952–961.

Bau, M., Koschinsky, A., Dulski, P. and Hein, J. R. (1996) Comparison of the partitioning behaviours of yttrium, rare-earth elements, and titanium between hydrogenetic marine ferromanganese crusts and seawater. *Geochim. Cosmochim. Acta* **60**, 1709–1725.

Bau, M., Usui, A., Pracejus, B., Mita, N., Kanai, Y., Irber, W. and Dulski, P. (1998) Geochemistry of low-temperature water-rock interaction: Evidence from natural waters, andesite, and iron-oxyhydroxide precipitates at Nishikinuma iron-spring, Hokkaido, Japan. *Chem. Geol*. **151**, 293–307.

Bolhar, R., Kamber, B. S., Moorbath, S., Fedo, C. M. and Whitehouse, M. J. (2004) Characterisation of early Archaean chemical sediments by trace element signatures. *Earth Planet. Sci. Lett*. **222**, 43–60.

Bolton, B. R., Exon, N. F., Ostwald, J. and Kudrass, H. R. (1988) Geochemistry of ferromanganese crusts and nodules from the South Tasman Rise, southeast of Australia. *Mar. Geol*. **84**, 53–80.

Byrne, R. H. (2002) Inorganic speciation of dissolved elements in seawater: The influence of pH on concentration ratios. *Geochem. Trans*, **3**, 11–16.

Byrne, R. H. and Kim, K. H. (1990) Rare earth element scavenging in seawater. *Geochim. Cosmochim. Acta* **54**, 2645–2656.

Byrne, R. H. and Lee, J. H. (1993) Comparative yttrium and rare-earth element chemistries in seawater. *Mar. Chem*. **44**, 121–130.

Chester, R. and Hughes, M. J. (1967) A chemical technique for the separation of ferro-manganese minerals, carbonate minerals and adsorbed trace elements from pelagic sediments. *Chem. Geol*. **2**, 249–269.

Davranche, M., Pourret, O., Gruau, G. and Dia, A. (2004) Impact of humate complexation on the adsorption of REE onto Fe oxyhydroxide. *J. Colloid. Interface Sci*. **277**, 271–279.

Davranche, M., Pourret, O., Gruau, G., Dia, A. and Le Coz-Bouhnik, M. (2005) Adsorption of REE(III)-humate complexes onto MnO_2: Experimental evidence for cerium anomaly and lanthanide tetrad effect suppression. *Geochim. Cosmochim. Acta* **69**, 4825–4835.

Davranche, M., Pourret, O., Gruau, G., Dia, A., Jin, D., and Gaertner, D. (2008) Competitive binding of REE to humic acid and manganese oxide: impact of reaction kinetics on development of Cerium anomaly and REE adsorption. *Chem. Geol*. **247**, 154–170.

De Carlo, E. H., Wen, X.-Y. and Irving, M. (1998) The influence of redox reactions on the uptake of dissolved Ce by suspended Fe and Mn oxide particles. *Aquatic Geochem*. **3**, 357–389.

Elderfield, H. (1988) The oceanic chemistry of the rare earth elements. *Phil. Trans. Roy. Soc. London A* **325**, 105–126.

Haley, B. A., Klinkhammer, G. P. and McManus, J. (2004) Rare earth elements in pore waters of marine sediments. *Geochim. Cosmochim. Acta* **68**, 1265–1279.

Hein, J. R., Koschinsky, A., Halbach, P., Manheim, F. T., Bau, M., Kang, J.-K. and Lubick, N. (1997) Iron and manganese oxide mineralizations in the Pacific. *Manganese Mineralizations: Geochemistry of Terrestrial and Marine Deposits* (Nicholson, K., Hein, J. R., Bühn, B. and Dasgupta, S., eds.), *Geol. Soc. Spec. Publ*. **119**, 123–138.

Hunter, K. A. (1991) Surface charge and size spectra of marine particles. *Marine Particles: Analysis and Characterization* (Hurd, D. C. and Spencer, D. W., eds.), *Geophys. Monogr*. **63**, 259–262.

Hunter, K. A. and Liss, P. S. (1979) The surface charge of suspended particles in estuarine and coastal waters. *Nature* **282**, 823–825.

Hunter, K. A. and Liss, P. S. (1982) Organic matter and the surface charge of suspended particles in estuarine waters. *Limnol. Oceanogr*. **27**, 322–335.

Kawabe, I., Ohta, A. and Miura, N. (1999a) Distribution coefficients of REE between Fe oxyhydroxide precipitates and NaCl solutions affected by REE-carbonate complexation. *Geochem. J*. **33**, 181–197.

Kawabe, I., Ohta, A., Ishii, S., Tokumura, M. and Miyauchi, K. (1999b) REE partitioning between Fe–Mn oxyhydroxide precipitates and weakly acid NaCl solutions: Convex tetrad effect and fractionation of Y and Sc from heavy lanthanides. *Geochem. J*. **33**, 167–179.

Koeppenkastrop, D. and De Carlo, E. H. (1992) Sorption of rare earth elements from seawater onto pure mineral phases: An experimental approach. *Chem. Geol*. **95**, 251–263.

Koeppenkastrop, D. and De Carlo, E. H. (1993) Uptake of rare earth elements from solution by metal oxides. *Environ. Sci. Technol*. **27**, 1796–1802.

Koschinsky, A. and Halbach, P. (1995) Sequential leaching of marine ferromanganese precipitates: genetic implications. *Geochim. Cosmochim. Acta* **59**, 5113–5132.

Koschinsky, A. and Hein, J. R. (2003) Acquisition of elements from seawater by ferromanganese crusts: Solid phase associations and seawater speciation. *Mar. Geol*. **198**, 331–351.

Kuhn, T., Bau, M., Blum, N. and Halbach, P. (1998) Origin of negative Ce anomalies in mixed hydrothermal-hydrogenetic Fe–Mn crusts from the Central Indian Ridge. *Earth Planet. Sci. Lett*. **163**, 207–220.

Li, Y.-H. (1981) Ultimate removal mechanisms of elements from the ocean. *Geochim. Cosmochim. Acta* **45**, 1659–1664.

Li, Y.-H. (1982) Interelement relationship in abyssal Pacific ferromanganese nodules and associated pelagic sediments. *Geochim. Cosmochim. Acta* **46**, 1053–1060.

Li, Y.-H. (1991) Distribution patterns of the elements in the ocean: A synthesis. *Geochim. Cosmochim. Acta* **55**, 3223–3240.

Liu, X. and Byrne, R. H. (1998) Comprehensive investigation of yttrium and rare earth element complexation by carbonate ions using ICP-mass spectrometry. *J. Sol. Chem*. **27**, 803–815.

Manceau, A., Gorshkov, A. and Drits, V. A. (1992) Structural chemistry of Mn, Fe, Co, and Ni in manganese hydrous oxides: Part II. Information from EXAFS spectroscopy and electron and X-ray diffraction. *Am. Mineral*. **77**, 1144–1157.

Masuda, A., Kawakami, O., Dohmoto, Y. and Takenaka, T. (1987) Lanthanide tetrad effects in nature: two mutually

opposite types, W and M. *Geochem. J.* **21**, 119–124.
McLennan, S. M. (1989) Rare earth elements in sedimentary rocks: influence of provenance and sedimentary processes. *Geochemistry and Mineralogy of the Rare Earth Elements* (Lipin, B. R. and McKay, G. A., eds.), *Rev. Mineral.* **21**, 169–200.
Moffett, J. W. (1990) Microbially mediated cerium oxidation in seawater. *Nature* **345**, 421–423.
Moffett, J. W. (1994) A radiotracer study of cerium and manganese uptake onto suspended particles in Chesapeake Bay. *Geochim. Cosmochim. Acta* **58**, 695–703.
Moorby, S. A. and Cronan, D. S. (1981) The distribution of elements between co-existing phases in some marine ferromanganese-oxide deposits. *Geochim. Cosmochim. Acta* **45**, 1855–1877.
Neihof, R. A. and Loeb, G. I. (1972) The surface charge of particulate matter in seawater. *Limnol. Oceanogr.* **17**, 7–16.
Ohta, A. and Kawabe, I. (2000) Rare earth element partitioning between Fe oxyhydroxide precipitates and aqueous NaCl solutions doped with $NaHCO_3$: Determinations of rare earth element complexation constants with carbonate ions. *Geochem. J.* **34**, 439–454.
Ohta, A. and Kawabe, I. (2001) REE(III) adsorption onto Mn dioxide (δ-MnO_2) and Fe oxyhydroxide: Ce(III) oxidation by (δ-MnO_2). *Geochim. Cosmochim. Acta* **65**, 695–703.
Quinn, K. A., Byrne, R. H. and Schijf, J. (2004) Comparative scavenging of yttrium and the rare earth elements in seawater: Competitive influences of solution and surface chemistry. *Aquatic Geochem.* **10**, 59–80.
Quinn, K. A., Byrne, R. H. and Schijf, J. (2006a) Sorption of yttrium and rare earth elements by amorphous ferric hydroxide: Influence of solution complexation with carbonate. *Geochim. Cosmochim. Acta* **70**, 4151–4165.
Quinn, K. A., Byrne, R. H. and Schijf, J. (2006b) Sorption of yttrium and rare earth elements by amorphous ferric hydroxide: Influence of pH and ionic strength. *Mar. Chem.* **99**, 128–150.
Quinn, K. A., Byrne, R. H. and Schijf, J. (2007) Sorption of yttrium and rare earth elements by amorphous ferric hydroxide: Influence of temperature. *Environ. Sci. Technol.* **41**, 541–546.
Tessier, A., Campbell, P. G. C. and Bisson, M. (1979) Sequential extraction procedure for the speciation of particulate trace metals. *Anal. Chem.* **51**, 844–850.
Usui, A. and Someya, M. (1997) Distribution and composition of marine hydrogenetic and hydrothermal manganese deposits in the northwest Pacific. *Manganese Mineralizations: Geochemistry of Terrestrial and Marine Deposits* (Nicholson, K., Hein, J. R., Bühn, B. and Dasgupta, S., eds.), *Geol. Soc. Spec. Publ.* **119**, 177–198.
Verplanck, P. L., Nordstrom, D. K., Taylor, H. E. and Kimball, B. A. (2004) Rare earth element partitioning between hydrous ferric oxides and acid mine water during iron oxidation. *Appl. Geochem.* **19**, 1339–1354.
Zhang, J. and Nozaki, Y. (1996) Rare earth elements and yttrium in seawater: ICP-MS determinations in the East Caroline, Coral Sea, and South Fiji basins of the western South Pacific Ocean. *Geochim. Cosmochim. Acta* **60**, 4631–4644.